International Journal of Engineering Innovation & Research
Volume 4, Issue 3, ISSN: 2277 – 5668

Change Detection in Terrestrial Laser Scanner Data Via Point Cloud Correspondence

M.Tsakiri, V. Anagnostopoulos
School of Rural and Surveying Engineering, National Technical University of Athens, Greece

Abstract **– Terrestrial laser scanning (TLS) is gaining much interest in the engineering community as a tool used to track changes in natural or object surfaces in 3D at an unprecedented resolution and precision. Unraveling surface change in this context requires the comparison of measurements of the same surface at different time periods. In this paper, it is discussed how TLS data can be used in change detection of small magnitude (up to few cm) via direct point cloud comparison. The strategy includes point cloud data acquired at multiple epochs, then referenced into a common coordinate system and applying 3D point correspondence to detect the surface changes. Four different algorithms, namely the nearest neighbour, nearest neighbour with local modelling, normal shooting and iterative closest point (ICP) are examined. A comparison of the performance of the algorithms is given with a validation experiment where a deformation measurement scenario was simulated. The study has shown that the most consistent results are provided by the nearest neighbour with local modelling and the ICP algorithms.**

Keywords **– Geomatics, Terrestrial Laser Scanning, Change Detection, Point Cloud Comparison.**

I. INTRODUCTION

Change detection is the process of identifying differences in the state of an object or phenomenon by observing it at different times [1]. Change detection is useful in many diverse applications, from large scale such as land use change analysis, disaster monitoring, environmental modelling, to smaller scale such as damage assessment of building infrastructure, stress detection in engineering structures, deformation of small objects etc. Change detection techniques have been developed for decades mainly for large-scale applications using remote sensing data. Automatic detection of changes with airborne photogrammetry or airborne laser scanning (ALS) is also widely researched (e.g. [2], [3]). The behaviour of small size natural phenomena or changes of specific objects are of great importance for analyzing deformations or an object's evolution, and require a more subtle measurement technique and data analysis. In this area, terrestrial laser scanning (TLS) with the prominent advantages of remote and non-contact collection of 3D measurements for direct surface description (point clouds) and high speed data acquisition at the few millimetre level has made it a very suitable data collection tool for the general 3D change detection problem. For further details on TLS the reader may refer to a number of textbooks such as [4], [5], [6].

Concerning the change detection via point clouds, several ways have been proposed in recent years to categorise the various approaches from different perspectives. In [1] two categories are defined, i.e. classification-based comparison and direct comparison of raw multi-temporal data. The former approach finds implementation to point clouds usually acquired from airborne platforms such as ALS. Based on this approach, ALS point clouds are converted to digital surface models (DSM) and then are classified in 2.5D. This also works for Triangulated Irregular Networks (TINs) or other surface representations. The DSMs are subtracted to identify changes (e.g. [7], [8]). Some researchers classify point clouds directly in 3D as urban objects, e.g. buildings, trees, and then detect the changes in 3D [9]. Another approach is to compare a base map with the acquired ALS data set but for TLS data sets, this is not so straight forward. The main reason is that TLS data are considered as unstructured 3D representation, whereas ALS data are regarded as 2.5D.

The second approach, in which raw data are directly compared, has been mostly used in point clouds acquired from terrestrial platforms (TLS and mobile laser scanners MLS). The main methods found in the literature to detect changes are by a) using visibility query, and b) point cloud subdivision. By using visibility query methods, two scans are compared directly via range image subtraction. Specifically, when the clouds are co-aligned (or registered to a common reference coordinate system), a pixel at a given location in both scans has a common ranging direction. Thus, implementing the change detection is equivalent to asking whether a point measured in the analyzed scan can be seen from the reference scanner position [10]. In methods of point cloud subdivision, two scans are compared directly using segmentation structures (such as octree, kdtree etc) for accessing the 3D point cloud and measuring the changes via some metric space such as the Hausdorff distance. The Hausdorff metric, measures how far two compact non-empty subsets of a metric space are from each other and is often used in computer vision. In [11] a point-to-point comparison was implemented by using the Hausdorff distance as a measure for changes. Whilst methods (a) apply for change detection of scenes in the order of several meters, methods (b) apply usually to change detection of smaller size objects and surfaces (i.e. order of cm).

As mentioned earlier, during the change detection, not only objects or areas in the point cloud are identified where changes have occurred but there is also the possibility to perform a deformation analysis. The available deformation methods can be divided in three different categories: (i) point-to-point-based methods, (ii) point-to-surface-based methods, (iii) surface-to-surface-

based methods. The first category uses the direct comparison of the 3D coordinates of discrete identical points recognised in the point clouds. These points are scattered on the surface of the object in the form of targets (such as reflective planes or spheres). The centre point coordinates can be calculated by a best fit algorithm and the coordinates are introduced in a classical deformation analysis using identical points. The disadvantage is the use of artificial targets which can be laborious to place them on the scanned area. Secondly, only a very small part of the redundancy contained in overlapping scans is used for the calculation and the resulting accuracy of the orientation parameters is therefore insufficient for detecting deformations (e.g. [12], [13]. In the second category, one of the point clouds is represented by a surface (usually the reference point cloud using tessellation such as TIN, implicit or explicit functions such as Non-Uniform B-Spline, NURBS) and for a point in the second point cloud the distance to the surface is calculated (e.g. [14], [15], [16]). The third category comprises methods of computing the distance between two surfaces calculated from the point clouds (e.g. [17], [18], [19]).

The behaviour of small size changes of specific objects are of great importance for analyzing deformations or object evolution, and require a more subtle analysis of the measured scene (e.g. [20]). Inspired by the idea of direct comparison of two partially overlapping clouds of the same object and measuring the changes via some metric space, this paper examines four different algorithms which detect and quantify changes (in the order of few mm) via point cloud correspondence. These algorithms are namely, the nearest neighbour, nearest neighbour with local modelling, normal shooting and iterative closest point (ICP), and operate directly on point clouds without requiring to need of creating surfaces such as TINs. Prior to the direct comparison of the two point clouds a segmentation structure is implemented (such as octree, k-d tree etc) for accessing the 3D point cloud. Although many authors have evaluated the accuracy of the above algorithms independently, few provide a comparison between them (e.g. [21], [22]). An additional goal of the paper is not only to present a comparative study regarding the algorithms for the detection of changes but also to propose an efficient solution aware of the unique characteristics of the TLS data.

The paper is structured in four sections. The second section describes the processing workflow for direct point cloud comparison and Section 3 describes briefly the different algorithms that were implemented in this work. Section 4 presents the experimental test data for a simulated surface and a designated object and gives a comparison of the performance between the four algorithms. It is mentioned here that this paper deals with small changes in the order of few mm up to few cm found in smooth manmade surfaces (of about 3-4m^2 of area). Such an application can find its use in static scenes when reconstructing for example, cultural heritage objects or engineering related objects such as metal tanks. Finally a discussion on the results is given and the main conclusions are drawn.

II. WORKFLOW FOR CHANGE DETECTION

The workflow of the procedure in order to detect changes directly for two point clouds collected at different epochs is shown in Fig. 1. At this point, it is necessary to define the difference between changes and deformations. In the surveying engineering terminology, changes are considered as differences in the state of an object, whereas deformations are small differences in the shape of an object. However, a large deformation can be regarded as a change, while a small change can be a deformation. In this work, the surface changes are small (less than 10cm) and are regarded also as a deformation. Therefore, in the remainder of the paper, change and deformation will be regarded the same.

The first step in the workflow involves the data acquisition from the TLS. The most typical use of scanning involves multiple setups (n scans) from different viewpoints in order to capture complex objects or setups at different epochs to capture the same object. But TLSs measure the positions of points with reference to their internally defined sensor frame. Thus, prior to any other processing, these individual datasets must be transformed and registered from their respective internal systems into an externally defined system (e.g. [23]).

Registration allows the estimation of the rigid transformation parameters (rotation and translation) to be determined in order to bring one dataset into alignment with the other in order to accurately define all scans in a common coordinate system. This can be achieved using either (a) computer-based methods, or (b) geodetic methods. In the literature, one of the most popular computer methods is the ICP (Iterative Closest Point) algorithm and its variants ([24], [25]). Other computer-based popular approaches use surface matching algorithms (e.g. [19]) allowing pair-wise co-registration of scans on the basis of a shared portion of the captured surface. The surveying methods rely on target-based registration with the disadvantage of the geodetic measurements introducing some errors, which might exceed the internal error of the scanner instrument (e.g. [26]).

The next step is the georeference of the registered point clouds collected at two epochs. Because the registration is performed per epoch, all epochs must be referred to the same coordinate system. The coordinate system of an epoch, usually the first, is considered as the "reference epoch" and the remaining epochs are georeferenced with respect to this epoch. The core of the workflow is the direct comparison of the two georeferenced clouds obtained at different epochs. This is performed using a point cloud correspondence approach. Other researchers use different approaches such as segmentation whereby subsets of the point cloud are formed by grouping points with similar properties under a given homogeneity criterion (e.g. [27], [16]). However, segmentation is a non-trivial problem because an absolute definition of a 'good' segment does not exist and very often within the same

point cloud features are best represented by segments with differing geometric or radiometric characteristics. Also, a major problem with surface based segmentation is the presence of noise in point clouds and the structure of the cloud which is not compact compared to other structures such as TINs (e.g. [28]). The algorithms used in this work to perform the point cloud correspondence are described in the following section. The data structuring implemented for the point correspondence is typically achieved by means of tree structures such as the octree [29] and k-d trees [30].

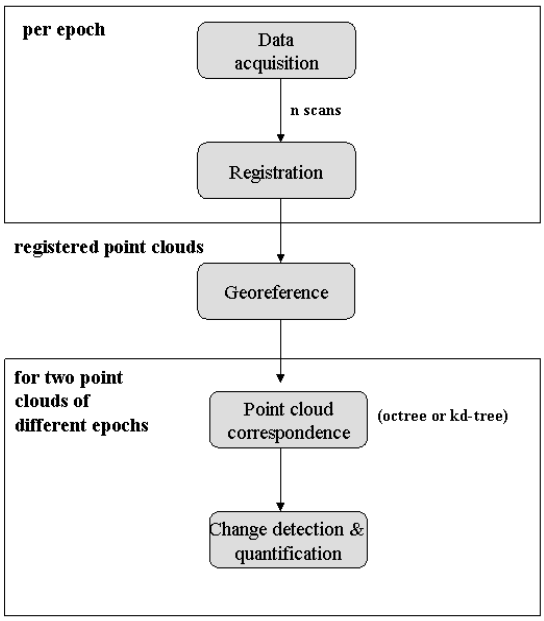

Fig. 1. Overview of workflow.

III. Point Correspondence Algorithms

This paper examines four different algorithms which detect and quantify changes (in the order of few mm) via point cloud correspondence. These are the (a) nearest neighbour, (b) nearest neighbour with local modelling, (c) normal shooting and (d) iterative closest point (ICP). The first three are categorised as global matching algorithms and the ICP is a local-search algorithm. Below there is a brief description of each algorithm.

A. Nearest-neighbour distance

The simplest way to compare two clouds is the algorithm of the "nearest" neighbour search (NNS)" and its variants, which effectively calculates the closest (or most similar) points. Formally, the nearest-neighbour search problem is defined as follows: Let $P = \{\vec{p}_i\}_1^n$ be a set of n points in a d-dimensional space and $\vec{q}$ be a query point. The nearest-neighbour search problem states: Find the point $\vec{p}_C$ in P which is the minimum distance from $\vec{q}$, i.e., $\|\vec{q} - \vec{p}_C\| \leq \|\vec{q} - \vec{p}_i\| \ \forall \vec{p}_i \in P$. The algorithm for each point i in the compared cloud $(X_i^{comp}, Y_i^{comp}, Z_i^{comp})$ searches its nearest neighbour j in the reference cloud $(X_j^{ref}, Y_j^{ref}, Z_j^{ref})$. When this is located , the Euclidean distance $\|u_i\|$ between both points is computedSubmit your manuscript electronically for review.

$$u_i = \begin{pmatrix} \Delta X_i \\ \Delta Y_i \\ \Delta Z_i \end{pmatrix} = \begin{pmatrix} \Delta X_i^{ref} \\ \Delta Y_i^{ref} \\ \Delta Z_i^{ref} \end{pmatrix} - \begin{pmatrix} \Delta X_j^{comp} \\ \Delta Y_j^{comp} \\ \Delta Z_j^{comp} \end{pmatrix} \quad (1)$$

B. Nearest neighbour with local modeling

The nearest neighbour distance approach is virtually assumption-free, but its results can be quite unstable especially when the two compared point clouds are insufficiently dense. A better approach is this case is to use nearest neighbour with surface modelling algorithms. Instead of directly comparing the points between the two clouds, a comparison is performed via a local surface created by a number of nearest points. Then the calculation of the distance from each point of the compared cloud is compared not with the nearest point, but with the projection of the surface that has been computed. Statistically this methodology is more accurate and not so dependent on the density of the cloud, but it can sometimes produce abnormal results due to the fact that the modelling of the cloud is limited (only a small number of local points are used and small errors remain especially for curved or angled surfaces). It does, though, give much better results on a global scale [11]. The mathematical surfaces that can be used are numerous. The only constraint factor in selecting a mathematical surface is the computational time for the calculation of the surface. Thus mathematical surfaces should be simple such as a plane or a low level polynomial function. In this work three surfaces were used: plane, triangulation, and polynomial function (see Table 1).

C. Normal shooting

The original algorithm [25] is defined as finding the intersection of the ray originated at the source point in the direction of the source point's normal with the destination surface. The variant algorithm implemented in this work finds the closest point in the destination cloud instead. Therefore, for the calculation of changes or deformations, for each point in the reference cloud the normal vector to the point is calculated. Among the k closest neighbours in the compared cloud, the point which has the shortest perpendicular distance is considered the corresponding point to the reference cloud and the Euclidean distance between the two points is computed.

D. ICP algorithm

An alternative way of detecting changes and small deformations is the use of the registration-based methods, with the most popular being the algorithm of ICP. Since its conception [24], a large number of variants have been developed and a good survey of different variations of ICP is presented in [31]. Using this approach, the detection is not performed on a global basis but the cloud is segmented into smaller areas.

Initially, the algorithm requires the data set of the whole area and gives an estimation of the average deformation, but often the deformation is not uniform to the whole area surface. In the process of locating localized deformations, the scanned area is segmented in smaller regions where the

ICP algorithm is applied in the pair of the corresponding segments. In the algorithm implemented in this work, an octree is used which segments the compared cloud in cubic areas with specific size. To the points which are inside the cube the ICP is applied and a vector between the initial and the final position is calculated (e.g. [32]).

The advantage of this methodology over the others is that it is less prone from errors due to the noise of the measurements because it takes into account not only one point in the cloud but all the points which are inside the sub-cube, so it calculates an average of deformation on these points. Therefore it is suitable for more noisy clouds. The main drawbacks of the algorithm are the problems that are often seen in the convergence of the algorithm to a correct solution which is not always guaranteed and the intensive calculations and therefore may not be suitable for the calculation of deformation of large areas.

IV. IMPLEMENTATION EXPERIMENTS

All the algorithms were examined using synthetic and real data. In the following a detailed description is given.

A. *Parameters of search-space*

The following table (Table 1) summarises some basic properties of the algorithms that were implemented in this work and the data structure used. A parameter that influences the performance of the algorithms is the maximal distance parameter, which restricts the search space around the query point, because the larger the maximal distance the more of the space the search routine must explore. For this reason, different values of the search space were used for the normal shooting and the ICP in order to investigate possible effects.

Table 1. Parameters of search space in the implemented algorithms.

Algorithm	**Data structure**	**Variation of parameter**
Nearest neighbour (NN)	octree or k-d tree	True distance, k-neighbours
NN local modelling	k-d tree	least squares best fitting plane, 2D 1/2 Delaunay triangulation, quadratic height function
Normal shooting	k-d	(5, 10), (300, 10), (5, 300), (300, 50)
ICP	octree	Voxel size: 0.01m, 0.02m, 0.05m, 0.1m

For the nearest neighbour with local modelling three variants that affect the search space were tested, depending whether a plane, triangulation or polynomial function was used (i.e. least square best fitting plane, 2D 1/2 Delaunay triangulation and quadratic height function). The normal shooting algorithm is affected by two parameters, the former showing the number of points from which the normal is calculated. The latter is the number of the k closest neighbours in the compared cloud amongst which the algorithm tries to locate the point with the shortest perpendicular distance in order to compute the Euclidean distance between the two clouds. The values of the two aforementioned parameters suggested in the literature are usually small to allow for quick search. In all the experiments four different sets were used including some extremities in order to verify the algorithm performance, i.e. (5, 10), (300, 10), (5, 300), (300, 50). For the ICP algorithm, the parameter that refers to the search space is the the voxel size. This is related to the storage of point clouds within the octree or k-d tree implementation and refers to the maximal depth of the occupied volumes by the points [33]. The voxel size in the experimental data varied from small to large sizes (i.e. 0.01m, 0.02m, 0.05m, 0.1m).

B. *Experimental data*

All algorithms may introduce false correspondences caused by a number of factors, such as inaccurate transformation parameters due to erroneous registration, point sampling variations between scans, occlusion etc. This is a problem that has attracted attention for improvement from the 3D vision community (e.g. [10], [11]). In this work, three factors are examined which have influence on the quality of the point pairs in the tested algorithms. These are: point sampling, registration error and choice of reference epoch (Table 2). These parameters may create noise and in the presence of noise in the input data, it is easy to create poor correspondences between pairs of points (e.g. [21]). In the remainder of the paper, the measuring epochs t1 and t2 will be used. Epoch t1 indicates the initial or reference point cloud of a surface measured at the first time, and epoch t2 indicates the successive point cloud of the same surface. In order to compare the algorithms, synthetic data is used and finally experiments with real data are realized. The evaluation metrics that are used τo assess the algorithm performance is the mean and standard deviation.

Table 2. Examined parameters in the experiments.

Parameter	**Variation of parameter**
Point sampling	- same point density in clouds of epoch t1 and t2 - different point density in clouds of epoch t1 and t2
Registration error	- introduced error of few cm
Choice of reference epoch	- comparison of clouds from epoch t2 to epoch t1 - comparison of clouds from epoch t1 to t2

C. *Synthetic data*

The synthetic test scene comprises two point clouds t1 and t2 with dimensions 3m x 1.5m in X and Y-axis, respectively. In t1 cloud, the Z axis is equal to zero, i.e. zero deformation. The t2 cloud has changes/deformations of parabolic shape, varying from 5mm to 2cm, introduced on the Z axis only. Fig. 1 (a, b) illustrates these deformations by showing the differences between the two point clouds both in numerical and coloured scale. The data included no added noise for simplicity.

In the first scenario, the parameters were unchanged, ie same density point of 1mm in both clouds at t1 and t2, no registration error and comparison of clouds performed from epoch t2 to epoch t1 (cf. Table 2). All the algorithms detected the introduced changes successfully. The three algorithms also estimated the deformation with the expected metrics (i.e. mean equal to zero, standard deviation in the order of 1mm) but only the ICP gave different results (Fig. 2).

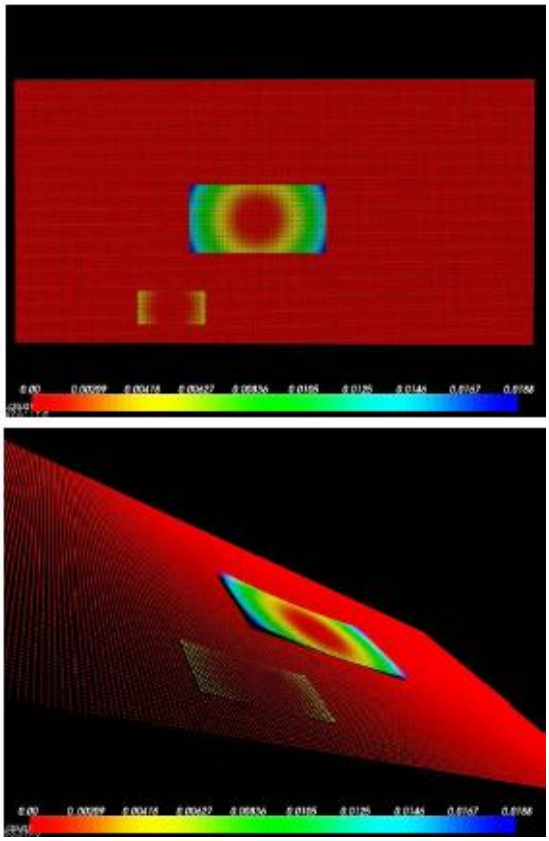

Fig. 1. Views of the synthetic point cloud data.

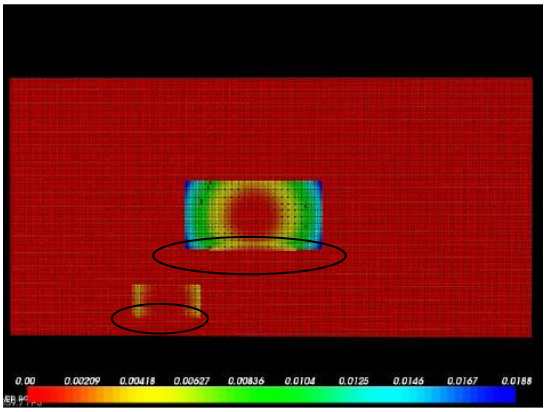

Fig.2. Detection with the ICP algorithm (voxel size 0.01m).

As seen in Fig.2, the algorithm could not detect correctly the changes at the bottom parts of the two parabolics. This is not unexpected because the ICP works better with noisy data. Also, if the number of points in the voxel is less than three it is possible that the ICP does not estimate the deformation correctly. In the next scenario, a comparison of point clouds from epoch t1 to epoch t2 was performed. Due to lack of noise there was no registration error and the density point variation could not exceed the 5mm as this is the size of the smallest introduced deformation. In this scenario, again all the algorithms detected the introduced changes successfully and the ICP performed with the same behaviour as in Fig. 2.

D. Real data

For the real data experiment the chosen object of testing is geometrically well defined (a satellite dish of diameter 1.4m) located inside the metrology laboratory of the School of Surveying Engineering in NTUA. The specific object has been measured with high accuracy industrial surveying techniques, thus knowing the 3D mathematical description of its surface with uncertainty in the sub-mm order. A terrestrial laser scanner (Leica Scanstation 2) was used to collect the point cloud data with the scanner-object distance during data acquisition always maintained within the quoted accuracy specifications of the manufacturer, i.e. 5-50m (hds.leica-geosystems.com). A number of scans were acquired with varying densities (1mm, 5mm, 10mm). The "change" (or deformation) on the object's surface was simulated through the use of children's plasticine placed on the scanned object. This material was used because is flexible, dense enough that it can retain its shape easily and does not melt under hot conditions. The simulated deformation from the moulded plasticine was in the form of different shapes, colours (white, blue, yellow) and sizes that varied from 0.3cm to 3.5cm. Three different placticine pieces with varying shape and colour were used: white with dimensions in length, width, height (4.3cm X 8.3cm X 09cm), blue with dimensions (13.5cm X 3.6cm) and height from 0.3cm to 2.2cm and yellow with dimensions (7.8cm X 7.2cm X 3.5cm) (Fig. 3). The epoch that the point clouds of the object without the plasticine were collected is considered as the reference epoch t1 and any subsequent clouds are considered as epoch t2, t3 etc.

Each epoch of measurements comprised three scans. Following the registration (which was achieved with an accuracy of 2mm), the georeferencing of the acquired clouds was performed externally, i.e. by using reflective targets measured by total station surveying with an accuracy of 1-2mm in order to avoid any influence due to the ICP algorithm at this stage (Fig. 4). The results of the algorithms were examined through the statistics of the mean and standard deviation of the change detection. Furthermore, the quality of the results was examined through the histogram of each algorithm run which classifies the deformation differences to classes. In the following histograms, the x-axis represents the measurement residuals and the y-axis the classes depending on the deformation differences.

The first testing scenario involved the parameters unchanged, ie same point density of 1mm in both clouds at t1 and t2, no registration error and comparison of clouds performed from epoch t2 to epoch t1 (cf. Table 2). The majority of the implemented algorithms and their

variations succeeded in detecting correctly the changes. Table 3 summarises the results of each algorithm by the mean and standard deviation of the change detection.

Fig.3. The simulated deformation by the moulded plasticine.

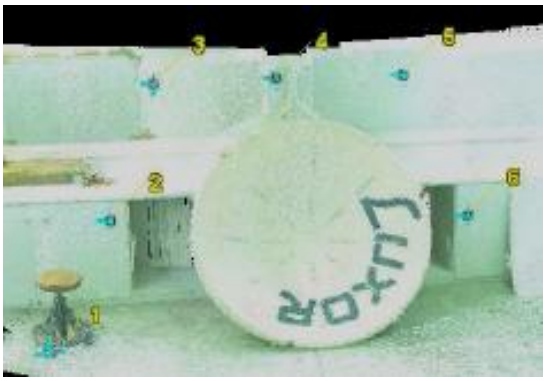

Fig.4. Registered point cloud with reflective targets for georeference.

Table 3. Statistics of results (testing scenario 1).

Algorithm	**Mean (m)**	**Stand. Deviation (m)**
NN	0.002	0.008
NN /local model. - plane - triangulation - quadratic	- 0.001 0.002 0.001	- 0.001 0.001 0.001
Normal shooting - (5, 10) - (5, 300) - (300, 10) - (300, 50)	- 0.003 0.010 0.002 0.002	- 0.002 0.008 0.001 0.001
ICP - (voxel 0.01)	0.001	0.000
- (voxel 0.02)	0.001	0.001
- (voxel 0.05)	0.001	0.000
- (voxel 0.1)	0.010	0.008

Only two variants, the Normal Shooting (5, 300) and the ICP (voxel 0.1m) gave slightly worse results Specifically, the algorithm of normal shooting gave unsatisfactory results when there were large number of nearest points on the compared cloud (i.e. 300) and small number of points (i.e. 5) from which the normal is calculated (Fig. 5a). Also the ICP algorithm failed to identify in detail the changes due to the large size of the voxel (Fig. 5b). When the ICP divides the space into large sub-cubes (voxels) it reduces the sensitivity of the algorithm making it more difficult to locate small deformations. When the voxel size was decreased, the results were better. This is also indicated in Table 1, where it can be seen that the majority of the algorithms produced a mean of less than 5mm which is within the noise level of the measurements. The plasticine colour had no effect at the obtained results.

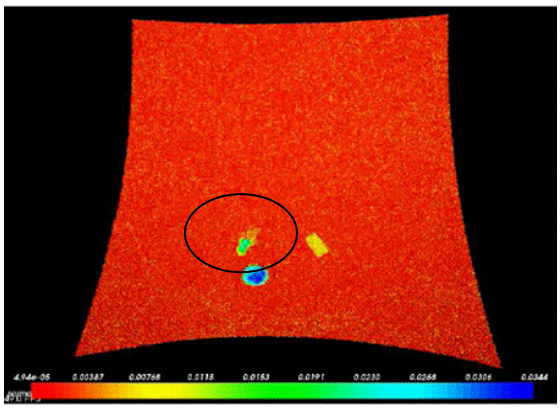

Fig. 5a. Erroneous detected changes by Normal shooting (5, 300).

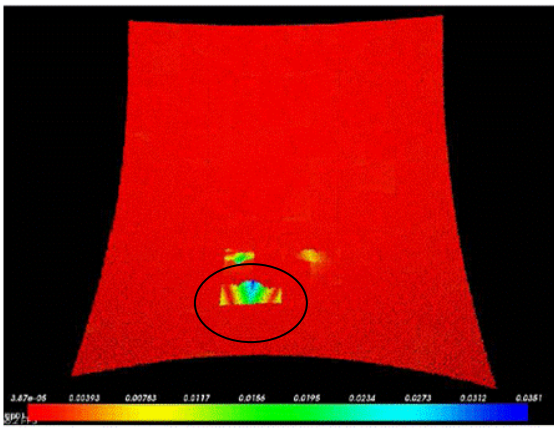

Fig.5b. Erroneous detected changes by ICP (voxel 0.1m).

The second testing scenario involved one parameter changed, the point density, and the other parameters unchanged, i.e. no registration error and comparison of clouds performed from epoch t2 to epoch t1 (cf. Table 2). The surface sampling or point density can be a case of misalignment for the algorithms. Theoretically when surfaces are scanned with low resolution, worse results are obtained. As surfaces have fewer points, point correspondences are found with low precision.

Specifically, the point clouds at t1 and t2 epochs had dissimilar point densities, varying from 1mm, 5mm and 10mm. At the tenfold level of difference (i.e., 10mm for the point cloud at t1 and 1mm for the cloud at t2) the algorithms could still detect the changes but the results were much noisier as indicated by the respective histograms (Fig.6).

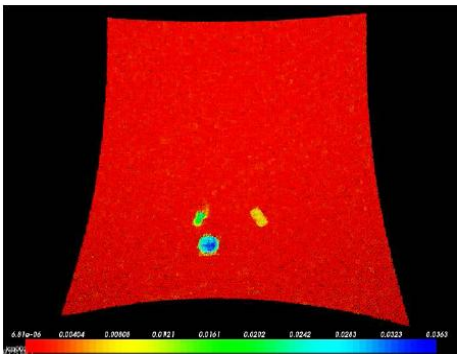

(a) Same point densities (1mm at t1 and t2 epochs).

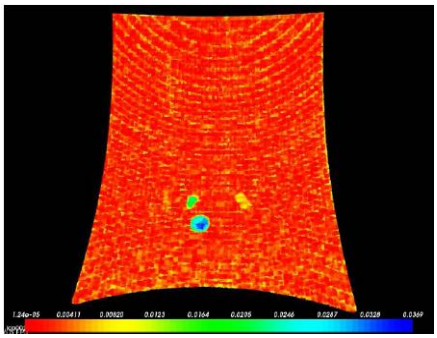

(b) Different point densities (10mm at t1, 1mm at t2).

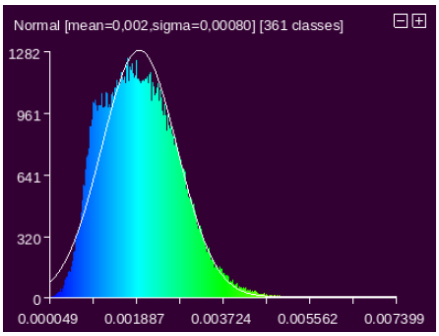

(c) Histogram of results using same point densities (1mm at t1 and t2 epochs).

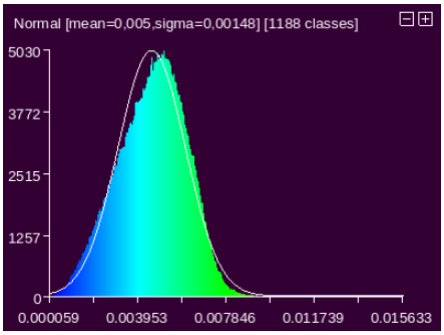

(d) Histogram of results using different point densities (10mm at t1, 1mm at t2)

Fig. 6. Results of the ICP algorithm (voxel 0.02m).

Fig. 6 depicts an example of the change detection performed by the ICP (voxel 0.002) and their respective histograms for when the point densities are the same in the two comparing clouds (Fig 6a, c) and for when the point densities are different, 10mm for the point cloud at t1 and 1mm for the cloud at t2 (Fig. 6b, d). Whilst the mean is in the same order (0.002m vs. 0.005m) as shown in Fig.6c, d, the standard deviation is affected (0.0008m vs. 0.0015m). The change in point density introduces higher noise in the point correspondence. In general, the results from all the algorithms showed that all point-to-point algorithms had slightly worse accuracy than point-to-plane algorithms because the plane interpolation decrements the effects of the sub-sampling with the NN algorithms having the best performance (i.e. low mean and standard deviation).

Table 4. Statistics of results (testing scenario 3).

Algorithm	**Mean (m)**	**Stand. Deviation (m)**
NN	0.004	0.00138
NN /local modelling - plane - triangulation - quadratic	- 0.002 0.004 0.003	- 0.00160 0.00153 0.00174
Normal shooting - (5, 10) - (5, 300) - (300, 10) - (300, 50)	- 0.006 0.010 0.004 0.004	- 0.00285 0.01152 0.00153 0.00152
ICP - (voxel 0.01)	 0.003	 0.00151
- (voxel 0.02)	0.003	0.00134
- (voxel 0.05)	0.005	0.00191
- (voxel 0.1)	0.006	0.00218

The third testing scenario involved one parameter changed, the registration between the two clouds, and the other parameters unchanged, i.e. same point density for clouds at t1 and t2 epochs and comparison of clouds performed from epoch t2 to epoch t1 (cf. Table 2). The registration of the point clouds is a significant parameter and can affect the detection of possible changes and can lead to false results.

As already mentioned, the initial registration was in the order of 2mm. At this experiment a deliberate error was introduced in one of the external targets that were used in the registration process. Thus, the resulting accuracy of the registration was 0.022m. It was noticed that all algorithms could not detect the change simulated by the white plasticine, meaning that changes below 1cm were undistinguishable (Fig.7). Fig. 7 presents an example of the change detection by the algorithms Normal Shooting (5, 300) and the ICP (voxel 0.02). These two algorithms were chosen because they had better statistics compared to the others, as seen in Table 4. As seen, the white placticine on the right has not been detected at all (Fig. 7a, b). As expected, the histograms are noisier (Fig. 7c, d) and the statistics of the executed algorithms are affected by the registration error.

The fourth testing scenario involved one parameter changed; the comparison of clouds was performed from epoch t1 to epoch t2. The other parameters remained unchanged, i.e. same point density for clouds at t1 and t2 epochs and no registration error (cf. Table 2).

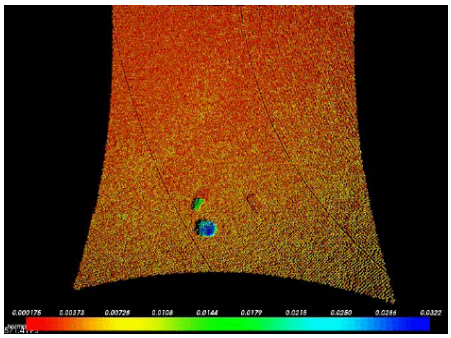

(a) Normal shooting (5, 300) with intentional error in registration.

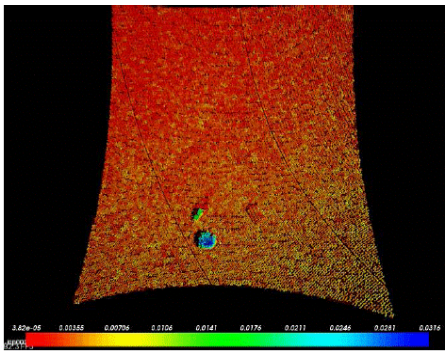

(b) ICP (voxel 0.02) with intentional error in registration.

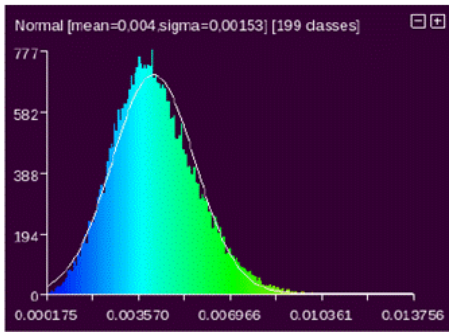

(c) Histogram of results using Normal shooting.

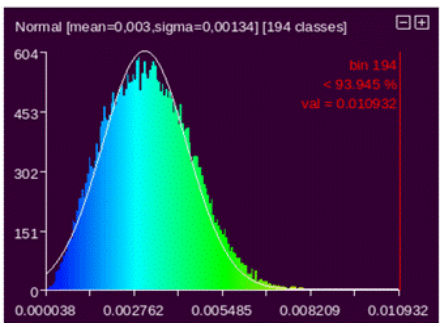

(d) Histogram of results using ICP.

Fig. 7. Example of the effect of registration error on two algorithms: Normal shooting and ICP.

The common approach in surveying applications for deformation detection involves the comparison from epoch t2 to epoch t1. Theoretically, there should be no differences in the absolute value of the results assuming that all other parameters of the experiments were kept identical (as in the first experiment). Whilst all the algorithms achieved detection of the simulated deformations, there were differences in the values compared to the respective results of the first testing scenario (cf. Table 2). The differences were observed in the detection of the plasticine of the biggest sizes. The largest differences were observed with the NN algorithms (Fig. 8) and were in the order of 1-2 mm (Fig. 9), while the normal shooting and ICP algorithms had insignificant differences.

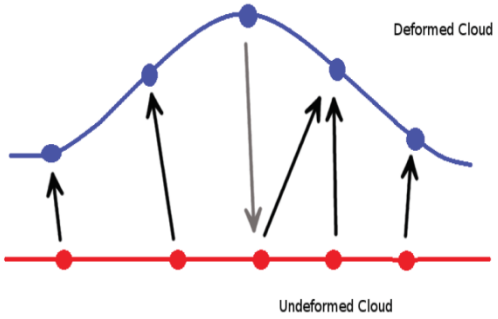

Fig. 8. Comparisons between deformed and undeformed point clouds using the NN approach.

Fig. 8 depicts schematically the behaviour of the NN approach. In the case of comparing the deformed (collected at epoch t2) with the undeformed cloud (collected at epoch t1) the nearest neighbour distance is calculated as shown by the grey coloured arrow. In the opposite case, the nearest neighbour distance is calculated as shown by the black coloured arrows. This is also shown in the results of Fig. 9 where the magnitude of the deformations is indicated by the coloured error bar. It is seen that the deformation of the section that has been circled in both 9(a) and 9(b) figures has been estimated differently with a maximum discrepancy of about 2mm. However, the smaller in size deformed areas did not exhibit the same differences by the NN algorithm.

Fig. 9 depicts schematically the behaviour of the NN approach. In the case of comparing the deformed (collected at epoch t2) with the undeformed cloud (collected at epoch t1) the nearest neighbour distance is calculated as shown by the grey coloured arrow. In the opposite case, the nearest neighbour distance is calculated as shown by the black coloured arrows. This is also shown in the results of Fig. 9 where the magnitude of the deformations is indicated by the coloured error bar. It is seen that the deformation of the section that has been circled in both 9(a) and 9(b) figures has been estimated differently with a maximum discrepancy of about 2mm. However, the smaller in size deformed areas did not exhibit the same differences by the NN algorithm.

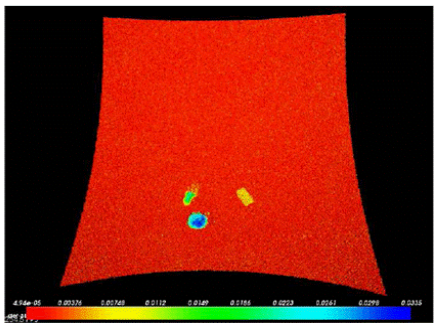

(a) Comparison between undeformed (epoch t1) with deformed (epoch t2) point clouds.

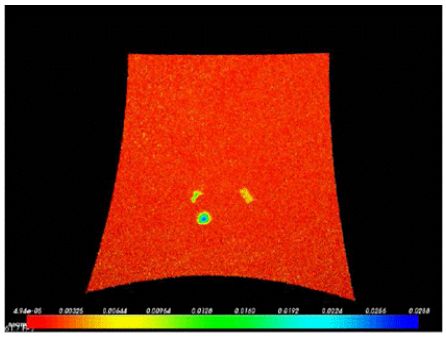

(b) Comparison between deformed (epoch t2) with undeformed (epoch t1) point clouds.

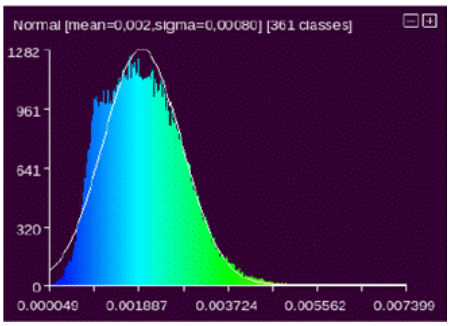

(c) Histogram of comparison results between undeformed (epoch t1) with deformed (epoch t2).

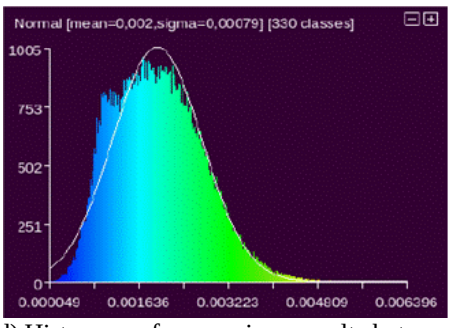

(d) Histogram of comparison results between deformed (epoch t2) with undeformed (epoch t1) point clouds.

Fig.9. Results using the NN algorithm between the deformed and undeformed point clouds.

V. DISCUSSION

From the results of both the simulated and real data it can be deduced that all algorithms were able to identify the changes. Consistently, the algorithm with the smallest errors was the NN/ local modelling and the ICP algorithms (for the ICP up to voxel size 0.05). Regarding the other algorithms, the NN algorithm is the simplest and the fastest but was inaccurate for small changes. It is also very dependent on the point density variations between scans as it does not consider any implicit or explicit surface, but only points. It can be used to provide a quick and rough evaluation of what has changed. The NN/local modelling algorithm offers better accuracy from the NN algorithm but is slower in terms of computing time. The Normal Shooting algorithm takes into consideration the geometrical characteristics of the object but introduces high levels of noise as it is very sensitive to point sampling variations between scans.

The NN/local modelling algorithm avoids any point sampling issues because it tries to model the surface locally. For each point of the first cloud, once the nearest point in the second cloud has been determined, a set of its nearest neighbours is extracted. With this set, a local surface model is computed (e.g. a least squares plane, a Delaunay triangulation, a spline surface etc) and the distance from the point of the first cloud to this surface patch is computed. The point-to-plane solutions were shown to be stable in all the experiments. This is expected because the overlap between the scans was kept high and the registration remained within few cm. These types of conditions are usual for laboratory experiments but are unlikely to happen in real applications. The ICP algorithm has shown to be the most robust to noise and density variations when compared to the aforementioned algorithms. The overall results propose that point-to-point (i.e. ICP variant used in this work vs. NN/local modelling) is slightly more accurate than point-to-plane solution (cf. Table 3).

From the simulated data results it was shown that the comparison of two data point cloud sets (i.e reference surface and deformed surface) requires that the size of the reference cloud should be at least the same or preferably larger from the deformed one. This is because the algorithms cannot distinguish between false point correspondence and real deformation at the borders of the clouds and may produce inaccurate results. Also, the point density of the reference cloud should be at least the same or preferably larger from the density of the deformed one as this may affect the search correspondence of the algorithms by introducing noise in the data.

The technical characteristics of the terrestrial laser scanner also can affect the accuracy of the estimated deformation. The sensor has two important features, noise and field of view, which can have an influence on the performance of the algorithm. Indeed, sensors with different noise levels may cope better with the algorithms or the one employed in this work may work better with variants of the examined algorithms. Furthermore, the

field of view and the point density profile of the sensor inside its field of view can have a huge influence on the algorithm performance as those characteristics govern the overlap and the possibility of multiple pairings between scans. For example, it was shown in this paper that it was not possible to detect changes or deformations below the single point precision of the scanner.

All the examined algorithms, as was shown in the third testing scenario, depend critically upon the accuracy of geometric registration of the two clouds. This is not unexpected because most existing algorithms expect a single model for the two surfaces being aligned. Such an assumption is good for practical reasons because the algorithms enable optimization to simultaneously find the best transformations for all points. However, a surface comprises different materials and may undergo different kinds of changes /deformation and in such cases multiple deformation models might be more useful. The main difficulties of doing so are the need for surface segmentation, constraints between adjacent models, and approaches to merge registration and deformation results. This requirement opens a future direction in this work.

VI. CONCLUSION

This work has presented a direct cloud-to-cloud comparison framework for change detection and has shown comparison tests for a number of algorithms. Experiments performed have shown the main characteristics of each algorithm and experimental results are reported to determine the best performance in the presence of noise and outliers, providing a useful guide for the interested user dealing with change/deformation (from few mm up to few cm) for small and smooth surfaces about 3-4m^2 of area.

In practice, all the examined algorithms gave similar results. Also, the overall results proposed that point-to-point algorithms gave slightly more accurate solutions than point-to-plane solutions with the latter being slightly more stable.

The comparative performance of the examined algorithms must be evaluated quantitatively in different environments and different surfaces, otherwise those interested in monitoring changes in a specific environment may not achieve the results obtained in the experiments shown here. In addition, a better analysis of the effects of various kinds of noise and distortion would yield further insights into the best algorithms for real-world, noisy scanned data.

REFERENCES

[1] A. Singh, "Digital change detection techniques using remotely-sensed data", I*nt. J. of Remote Sensing*, 10:6, 989-1003,1989 DOI: 10.1080/01431168908903939 .

[2] S. Xu, G. Vosselman, S. Oude Elberink, "Detection and classification of changes in buildings from airborne laser scanning data", Proc. *ISPRS Workshop Laser Scanning* 2013, 11 – 13 November, 2013, Antalya, Turkey.

[3] L. Matikainen, J. Hyyppä, H. Kaartinen, "Automatic detection of changes from laser scanner and aerial image data for updating building maps". Proc. *XXth ISPRS Congress*, July 2004, Istanbul, Turkey.

[4] G. Vosselman , HG. Maas, (eds), *Airborne and Terrestrial Laser Scanning*, 2010, ISBN-13: 978-1439827987.

[5] Y. Reshetyuk, *Terrestrial laser scanning: Error sources, self-calibration and direct georeferencing*. VDM Verlag July, 2009.

[6] J. Shan C.K. Toth, *Topographic Laser Ranging and Scanning: Principles and Processing*, Kindle Edition, 2008.

[7] J. Tian, P. Reinartz, P. d'Angelo, M. Ehlers " Region- based automatic building and forest change detection on cartosat-1 stereo imagery", *ISPRS J. of Photogrammetry and Remote Sensing* 79(0), 2013, pp. 226 – 239.

[8] H. Murakami, K. Nakagawa, T. Shibata, E.Iwanami, "Potential of an airborne laser scanner system for change detection of urban features and orthoimage development", *Int. Archives of Photogrammetry and Remote Sensing* 32, 1998, pp. 422–427.

[9] W. Xiao, B. Vallet, N. Paparoditis, "Change detection in 3D point clouds acquired by a mobile mapping system", *ISPRS Workshop Laser Scanning*, 11 – 13 November, 2013, Antalya, Turkey.

[10] R. Zeibak, S. Filin, "Change detection via terrestrial laser scanning", *ISPRS Workshop on Laser Scanning and SilviLaser* Espoo, September 12-14, 2007, Finland.

[11] D. Girardeau-Montaut, M. Roux, R. Marc, G. Thibault, "Change detection on points cloud data acquired with a ground laser scanner", *Int. Archives of Photogrammetry, Remote Sensing and Spatial Information Sciences* 36 (Part 3), 30–35, 2005.

[12] O. Monserrat, M. Crosetto, "Deformation measurement using terrestrial laser scanning data and least squares 3D surface matching", *ISPRS J. of Photogrammetry and Remote Sensing* 63 (1), 142–154, 2008.

[13] A. Abellán, J.M. Vilaplana, J. Calvet, D. Garcia-Selles, E. Asensio, "Rockfall monitoring by terrestrial laser scanning - case study of the basaltic rock face at Castellfollit de la Roca (Catalonia, Spain)" *Nat. Hazards Earth Syst. Sci.*, 11, 829–841, 2011.

[14] S.J.Gordon, D.D. Lichti, "Modelling terrestrial laser scanner for precise structural deformation measurement" *J. of Surveying Engineering* 133(2), 72-80, 2007.

[15] R. Van Gosliga, R. Lindenbergh, N. Pfeifer, " Deformation analysis of a bored tumnnel by means of terrestrial laser scanning", *Int. Archives of Photogrammetry, Remote Sensing and Spatial Information Sciences* 36(P5), 167-172, 2006.

[16] R. Lindenbergh, N. Pfeifer, "A statistical deformation analysis of two-epochs of terrestrial laser data of a lock", *7th Conf. on Optical 3D Measurement Techniques*, 3-5 Oct. 2005, Vol II, Vienna, Austria, 61-70.

[17] H-M. Zogg, H. Ingensand, "Terrestrial laser scanning for deformation monitoring - load tests on the felsanau viaduct", Proc., *ISPRS Congress*, 2008, pp 555-562.

[18] M. Alba, L. Fregonese, F. Prandi, M. Scaioni, P. Valgoi, "Structural monitoring of a large dam by terrestrial laser scanning", *Int. Archives of Photogrammetry, Remote Sensing and Spatial Information Sciences* 36 (part 5), 2006.

[19] A. Grün, D. Akca, "Least Squares 3D Surface Matching", *IAPRSSIS*, Vol. 34(5/WG16), 2004, Dresden, Germany.

[20] L. Truong-Hong, D.F. Laefer, "Using terrestrial laser scanning for dynamic bridge deflection measurement", *Istanbul Bridge Conference*, August 11-13, 2014, Istanbul, Turkey.

[21] F. Pomerleau, F. Colas, R. Siegwart, S. Magnenat, "Comparing ICP variants on real-world data sets- Open-source library and experimental protocol", *J. Auton. Robot*, 34:133–148 DOI 10.1007/s10514-013-9327-2, 2013.

[22] G. Dalley, P. Flynn, "Pair-wise range image registration: a study in outlier classification" *Comput. Vis. Image Und.*, 87 (1–3): 104–115, 2002.

[23] D.D. Lichti, J. Scaloud, "Registration and calibration", In: G. Vosselman and H.G. Maas (eds) *Airborne and terrestrial laser scanning*. Taylor and Francis, 2010.

[24] P. Besl, N. McKay, "A Method for Registration of 3-D Shapes" *Trans. PAMI*, 1992, 14(2).

[25] Y. Chen, G. Medioni, "Object modelling by registration of multiple range images", *Image and Vision Computing* 10(3): 145-155, 1992.

[26] J.-A. Paffenholz, *Direct geo-referencing of 3D point clouds with 3D positioning sensors*. PhD Thesis, Leibniz Universität Hannover, Germany, 2013.
[27] T. Rabbanni, F. van den Heuvel, G. Vosselman, "Segmentation of point clouds using smoothness constraint", *ISPRS Com. V Symp. 'Image Engineering and Vision Metrology*, September 25-27, 2006, Dresden, Germany, pp. 248-253.
[28] G. Sithole, W.T. Mapurisa, "3D object segmentation of point clouds using profiling techniques", *South African Journal of Geomatics*, 1(1):60-76, 2012.
[29] D. Meagher, "Geometric modeling using octree encoding", *Computer Graphics and Image Processing*, 19(2):129 – 147, 1982.
[30] J.L. Bentley, "Multidimensional Binary Search Trees Used for Associative Searching", *Communications of the ACM*, 18(9): 509– 517, 1975.
[31] S. Rusinkiewicz, M. Levoy, "Efficient Variants of the ICP Algorithm", *3rd Int. Conf. on 3D Digital Imaging and Modeling*, pp.145-152, DOI 10.1109/IM.2001.924423.
[32] T. Oppikofer, M. Jaboyedoff, L. Blikra, M.-H. Derron, R. Metzger, "Characterization and monitoring of the Aknes rockslide using terrestrial laser scanning", *Natural Hazards and Earth System Sciences*, 9:1003–1019, 2009.
[33] J. Elseberg, D. Borrmann, A. Nuchter, "One Billion Points in the Cloud —An Octree for Efficient Processing of 3D Laser Scans", *ISPRS Journal of Photogrammetry and Remote Sensing*, 2012,DOI:10.1016/j.isprsjprs.2012.10.004.

AUTHOR'S PROFILE

Maria Tsakiri

is currently an associate professor at the School of Rural and Surveying Engineering of the National Technical University of Athens (NTUA), Greece. She holds a PhD in geodesy from the University of Nottingham in UK. She has also held academic positions at Curtin University of Technology in Australia, School of Spatial Sciences.

Vassilios Anagnostopoulos

obtained his degree from the School of Rural and Surveying Engineering of the National Technical University of Athens (NTUA), Greece in 2013. He is currently completing an MSc course in Informatics at the University of Pireas, Greece and he will pursue a PhD at the University of Zurich ETH Switzerland commencing in September 2015.